Published in final edited form as:
Cancer. 2008 September 1; 113(5): 1032–1042. doi:10.1002/cncr.23678.

Hypoxia-regulated protein expression, patient characteristics, and preoperative imaging as predictors of survival in adults with glioblastoma multiforme

Jeannette R. Flynn, M.D.[1], **Libo Wang**[2], **David L. Gillespie, Ph.D.**[2], **Gregory J. Stoddard, M.P.H.**[3], **Jason K. Reid, B.S.**[2], **Jason Owens**[2], **Grant B. Ellsworth, B.S.**[2], **Karen L. Salzman, M.D.**[4], **Anita Y. Kinney, R.N., Ph.D.**[3], and **Randy L. Jensen, M.D., Ph.D.**[2]

[1]Center for Children, Huntsman Cancer Institute and Division of Pediatric Hematology/Oncology

[2]Department of Neurosurgery, University of Utah, Salt Lake City, Utah

[3]Department of Internal Medicine, University of Utah, Salt Lake City, Utah

[4]Department of Radiology, University of Utah, Salt Lake City, Utah

Abstract

Background—Regions of hypoxia within glioblastoma multiforme (GBM) tumors are common and may influence a tumor's aggressiveness, response to treatment, and the patient's overall survival. We examined four markers of hypoxia (HIF-1α, GLUT-1, VEGF, CA IX), cellular proliferation and microvascular density (MVD) indices, extent of surgical resection, and preoperative imaging characteristics and compared them with the overall survival rates of adults with GBM.

Methods—In this retrospective cohort study, patients with lower-grade astrocytomas were compared with a subset of patients with GBM to verify that our methods could establish differences between tumor grades. Using preoperative imaging, we established the amount of necrosis vs. overall tumor area. We also compared preoperative with postoperative images to define the amount of tumor resected. We compared molecular markers, proliferation, MVD, and imaging with survival of patients with GBM.

Results—The hypoxia-regulated molecules (HRMs) and indices for MVD and cellular proliferation were significantly associated with tumor grade. Survival was improved when ≥95% of the tumor was resected. Although the total tumor area was associated with overall survival, no differences were found when the amount of necrosis or a tumor necrosis index (area of necrosis/area of tumor) was compared with survival. We found that GLUT-1 and VEGF correlated with survival after controlling for age.

Conclusions—We differentiated tumor grade with HRMs, MVD, and proliferation but found GLUT-1 predicted survival in this group of patients with GBM tumors. These results suggest GLUT-1 may be an important independent prognostic indicator.

Keywords

HIF-1α; VEGF; GLUT-1; microvascular density; glioma; survival

Requests for reprints: Randy L. Jensen, M.D., Ph.D., Department of Neurosurgery, University of Utah, 175 N. Medical Drive East, Salt Lake City, UT 84132 Phone: 801-581-6908; Fax 801-581-4138; E-mail: randy.jensen@hsc.utah.edu.

INTRODUCTION

Glioblastoma multiforme (GBM) is the most common and most malignant brain tumor in humans. Despite resection and adjuvant treatment, the survival rates of patients who have GBM are only 3% and 1% at 5 and 10 years, respectively (Central Brain Tumor Registry of the United States, 2001 yearly report). Various hypoxia-regulated molecules (HRMs), as well as other factors such as cellular proliferation, angiogenesis, tumor necrosis, and extent of resection, have been compared with survival rates to identify those, either individually or in combination, that would aid in maximizing response to treatment or act as a prognostic indicator of improved survival.[1-3]

Regions of hypoxia within GBM tumors are common and may be a critical influence on tumor aggressiveness, response to treatment, and the patient's overall survival.[4-6] Molecular markers of hypoxia, including hypoxia inducible factor-1α (HIF-1α) and its downstream regulated targets vascular endothelial growth factor (VEGF), glucose transporter-1 (GLUT-1), and carbonic anhydrase nine (CA IX), have been evaluated, often separately or in limited combinations, for their ability to correlate with astrocytoma tumor grades and overall survival.[7-9] HIF-1 is a heterodimeric transcription factor that is thought to be the predominant regulator of oxygen homeostasis in cells.[10, 11] Overexpression of HIF-1α has been described in numerous cancers, including gliomas.[12] The specific role of HIF-1α in tumor growth is still not clear, but previous results suggest this transcription factor is necessary for proliferation and angiogenesis.[13] Overexpression has been found specifically in the perinecrotic zones that mark areas of avascularity and hypoxia.[14] We have previously demonstrated that HIF-1α inhibition using siRNA attenuates glioma growth in xenograph models, suggesting that it may play an important role in tumor growth.[15]

Intratumoral necrosis, angiogenesis, and cellular proliferation are histological features of GBM that have been shown to distinguish low-grade from high-grade gliomas.[4, 16-18] Conflicting results have been reported as to the efficacy of the use of cellular proliferation and microvascular density (MVD), which is used as a measure of the degree of angiogenesis, in predicting survival.[19-26]

Surgical management of GBM is important for tissue diagnosis but the role of radical resection has been less clear. GBM is a very infiltrative tumor, and "complete" resection is often not feasible. The degree of resection of enhancing tumor, however, has been associated with survival. In a very large series of patients with GBM, Lacroix et al. 40 found that the amount of tumor resected was associated with a survival advantage if ≥98% of the tumor was removed.

Although the correlation to survival of numerous factors has been investigated, it has been done using individual factors separately or combination with 1 or 2 others. In this study, we examine whether 4 cellular markers of hypoxia, proliferation and MVD indices, and extent of resection and tumor necrosis are predictors of overall survival in adults with GBM.

METHODS AND MATERIALS

Study Participants

After Institutional Review Board approval, we identified adults who had a GBM tumor from the senior author's tumor database. Adult patients who had a *de novo* GBM tumor, underwent resection/biopsy at the University of Utah, had tumor specimens available, and were deceased were included in the study. Patients with recurrent tumors, those who were still living or had no death documentation, and those for whom tissue samples had not been retained were excluded. Medical records were retrospectively reviewed for information

regarding age, sex, the location of the tumor, the extent of resection, treatment (radiotherapy and chemotherapy) received, specific imaging completed before and after resection, the length of progression-free survival (time from date of initial imaging to imaging documenting progression or recurrence), and length of overall survival (calculated from date of initial imaging to documented death from the Social Security Death Index). Patients with available preoperative and postoperative magnetic resonance (MR) imaging studies with and without contrast were identified, and their imaging studies were evaluated for tumor and necrotic area as well as the extent of resection as described below.

To document that the methods to evaluate HRMs, MVD, and proliferation would be valid, 10–12 randomly chosen patients within two additional tumor grades (low-grade gliomas [LGG]: WHO grade II; anaplastic astrocytomas [AA]: WHO grade III) were identified as control groups for comparison with our GBM (WHO grade IV) study group. No survival or treatment information was obtained on these patients with lower-grade tumors.

Immunohistochemistry

Immunohistochemistry was performed for HIF-1α, VEGF, GLUT-1, and CA IX using commercially available reagents according to manufacturer's recommendations. For HIF-1α, 4-μm thick sections of formalin-fixed, paraffin-embedded sections were dehydrated and dewaxed in graded alcohols. The Catalyzed Signal Amplification (CSA) Ancillary system (Dako) was used, following the manufacturer's protocol. The primary antibody was anti-HIF-1 (nb100-123, 1:1000). Lastly, 3,3'-diaminobenzidine (DAB) Chromogen solution (Vector Laboratories) was applied, and slides were counterstained in 0.1% toluidine blue. The slides were dehydrated in graded alcohols, dipped in 3 changes of xylene, and cover slipped.

For VEGF, GLUT-1, and CA IX immunohistochemical analysis, 4-μm thick sections of formalin-fixed, paraffin-embedded sections were deparaffinized in graded alcohols, heated with steam in citrate buffer (Unmasking Solution, Vector Laboratories) for 30 minutes, and treated with 3% H_2O_2. Using the Vectastain Rabbit Kit (Vector Laboratories) for the VEGF and GLUT-1, and Vectastain Goat Kit (Vector Laboratories) for CA IX, sections were incubated in blocking serum for 20 minutes and then overnight in a moist chamber with the respective primary antibodies. Then, after incubating for 30 minutes with diluted biotinylated antibody solution, the sections were incubated for 30 minutes in Vectastain ABC complex and processed using the DAB kit developing solution. Negative controls were performed by replacing the primary antibody with nonimmune serum, with all other steps performed as above. Positive controls for HIF-1, VEGF, GLUT-1, and CA-IX were performed on paraffin fixed sections of tumors grown in mice using human U251 cell lines, which are immunohistochemically positive for these proteins. The slides were then dehydrated in graded alcohols, dipped in 3 changes of xylene, and cover slipped.

All slides were examined using an Olympus BX41 Microscope. Under 200× (10 ocular × 20 objective) magnification, they were scored by a single investigator (R.L.J.) blinded to the specimen tumor grade or patient information. A score of 0–4 (0=0–25%, 1=25–50%, 2=50–75%, 3=75–100%, 4=100%) was given based on the number of cells stained in a given field.

Proliferation Index

To determine the proliferation index (PI), 4-μm thick slices of the slides were cut, melted at 55–60°C for 30 minutes, deparaffinized in xylene for 5 minutes, and rehydrated in graded alcohols for 1 minute each. Ki-67 (clone MIB-1) heat-induced epitope retrieval was applied in citrate buffer (pH 6.0) in an electric pressure cooker for 4 minutes. The following steps were performed on the Ventana ES (Ventana Medical Systems) at 40°C. The primary

antibody (dilution of 1:160) was soaked for 28 minutes and secondary antibody (dilution of 1:300) was soaked for 8 minutes (Mouse Fab, Dako). Detection was done using the IView DAB detection kit (Ventana), and the counterstain was done with hematoxylin (Ventana) for 4 minutes. Positive controls were performed on human thymus, which has a greater than 90% cell staining. Negative controls were performed by replacing the primary antibody with nonimmune serum, with all other steps performed as above. Slides were then dehydrated through graded alcohols for 30 seconds each, dipped in 4 changes of xylene, and cover slipped.

The PI was calculated by taking six random pictures representative of each slide at 400× (10 ocular × 40 objective) magnification using an Olympus Microfire camera. The pictures with the most and the least staining were discarded and the remaining 4 were analyzed. The images were transferred to Image-Pro Plus 5.0, and a LoPass large spectral filter was applied. Using the Count/Size measurement feature, the MIB-1-stained cells (brown) were counted with the manual intensity range selection tool by histogram-based segmentation. The background-stained cells (blue) were counted in the same manner. The PI was calculated as the number of MIB-1-stained cells divided by the total number of cells in the field ((# brown stained cells)/(# brown + # blue stained cells)). This was repeated 3 times for each picture and averaged. The results from all 4 pictures for each slide were averaged for the final PI (Fig. 1a,b). Analysis was duplicated by a separate researcher using a random subset of 20 slides. This method was very reproducible, as demonstrated by good inter-rater reliability (ρ=0.99, 95% CI(0.99–1.00)) and intra-rater reliability (ρ=0.96, 95% CI(0.92–0.99)).

MVD Index

The slides for the MVD index analysis were prepared using the same steps as described above for the MIB-1 analysis except that they were pretreated with Factor VIII (Rabbit polyclonal) Protease 2 (Ventana Medical Systems) for 4 minutes and the primary antibody (dilution of 1:100) was soaked for 32 minutes. The slides were then soaked in a secondary antibody (dilution of 1:300) for 8 minutes (Mouse Fab). Positive controls were performed on human tonsil. Negative controls were performed by replacing the primary antibody with nonimmune serum, with all other steps performed as above.

The MVD index was calculated based on a previously published method.27 Briefly, three pictures of the most vascular area of the slide, the ‘hotspot,’ were taken at 200× magnification using an Olympus Microfire camera. The pictures were then transferred to Photoshop CS 7 (Adobe Systems Incorporated), and any positive cell that was separate from other stained cells and not contiguous or branching from other vessels was counted. The results from all 3 pictures for each slide were averaged for the resulting MVD and divided by 0.26 mm^2 to normalize the size of the picture field.

Image analysis

Contrast-enhanced T1-weighted preoperative scans on patients with available MR imaging were uploaded using DicomWorks v1.3.5 and evaluated using a computer program developed by J.R. (MRI_2D). This Java program runs as a plug-in to the NIH imaging program, Image J, and is available upon request.

Each pixel in a MR image has an inherent value between 0 (black) and 255 (white). After the user clicks on an enhancing region of the tumor, the MRI_2D program performs an initial selection by moving from the clicked pixel outward to include all pixels that are within the initial default bounds (138–255; these initial default bounds were chosen during the set-up phase as selecting the majority of the enhancing tumors on numerous patient

samples). After MRI_2D performed the initial selection, the bounds were adjusted to include the entire region in question. These same numerical bounds were then used for all images from that patient (lower bound range=94–236, average=144). Necrotic regions are defined as regions within the tumor having a value of 0 to the bounds as they were defined above for the enhancing region (Fig. 1c,d). These regions of interest are used to calculate the total size of the tumor and area of necrosis in pixels. The ratio of necrosis area to tumor area is also calculated.

Statistical Analyses

Our sample size of GBM patients (n=62) provided 80% power to detect a hazard ratio of 2.1 in our Cox regression models, which was close to the effect size we anticipated. No formal sample size determination was undertaken for the three tumor groups, as the intention was simply to observe whether our methods could result in observable, but not necessarily statistically significant, differences.

The associations of tumor grade with the HRMs, which were measured as quartiles and treated as ordered categorical variables, were tested for significance using a categorical linear trend test. For pairwise comparisons of these markers between the tumor grade groups, a Wilcoxon-Mann-Whitney test was used, with adjustment for multiple comparisons using Holm's P-value adjustment procedure.28 An identical approach was taken with the continuous-scale molecular markers of MVD, and proliferation using these nonparametric tests, since there was a concern about meeting the normality assumption of a parametric approach given the small sample sizes.

Multivariable Cox regression was used to model time to death, adjusting for age as a potential confounder. Although linear regression could have been used, since all patients died, the Cox regression approach is still recommended as it provides more information and sensitivity. The proportional hazards assumption was tested for each predictor variable, both separately and globally, using a formal significance test based on the unscaled and scaled Schoenfeld residuals.29 The covariate age consistently violated the assumption and so was included as a time-dependent covariate to eliminate the need for proportional hazards on that covariate.

Age-adjusted Kaplan-Meier survival curves are reported. For these analyses, the predictor variables HRMs, PI, and MVD were divided at the median since the HRMs were ordered categorical variables with too few points in each category to provide reliable estimates. The other variables were continuous, but dividing at the median allowed the calculation of the hazard ratio that matched the Kaplan-Meier curves, where dividing at the median permitted two lines for visual comparison.

Statistical analyses were done using Stata 9.2 (StataCorp), using two-sided comparisons, with significance set at 0.05.

RESULTS

Patient population

One hundred and one patients with GBM tumors were initially identified; 39 were subsequently excluded (25 had recurrent tumors, 9 were still living, 2 had no death documentation available, and 3 had no available tissue) (Table 1). A subset of 42 patients with available MR imaging studies was identified (Table 1).

The randomly chosen control groups of patients with LGG and AA tumors included 12 and 10 patients, respectively. Demographic characteristics for these 2 groups were compared

with a randomly selected subset of patients with GBM (Table 2) and were not significantly different.

Tumor markers and tumor grade

To evaluate our ability to establish differences in HRMs, PI, and MVD between tumor grades, patient samples from the LGG, AA, and GBM groups were compared. All of the HRMs except CA IX increased significantly as the tumor grade increased (Fig. 2) (p-trend: 0.023, <0.001, 0.002, and 0.18 for HIF-1, GLUT-1, VEGF, and CA IX, respectively). Although the trend across tumor grades was significant, no pairwise comparisons of HIF-1α staining between tumor grades were significant after adjusting for multiple comparisons (LGG vs. AA, p=0.16; LGG vs. GBM, p=0.15; AA vs. GBM, p=0.27). However, when the GLUT-1 and VEGF staining for LGG were compared with those of AA (p=0.006 and 0.015, respectively) and GBM tumors (p<0.001 and p=0.011, respectively), the differences were highly significant. With CA IX, the trend across tumor grade was not significant and no differences were found (LGG vs. AA, p=0.10; LGG vs. GBM, p=0.41; AA vs. GBM, p=0.37). AA and GBM tumors frequently are grouped into a single ‘high-grade’ group and so it was not surprising that there were not significant differences found between these two groups throughout the HRMs (p=0.27, p=0.24, p=0.60, and p=0.37 for HIF-1, GLUT-1, VEGF, and CA IX, respectively) (Fig. 2e).

In our evaluation of MVD, significant differences were found between LGG and both AA and GBM tumors (p=0.027 and p=0.003, respectively) (Fig. 3a). No difference between AA and GBM was found (p=0.09). When comparing PI across tumor grades, significant differences were seen when GBM tumors were compared with LGG and AA (p=0.001 and p=0.038, respectively) (Fig. 3b). A significant difference was not seen when LGG tumors were compared with AA (p=0.19). The trends for both MVD and PI were significant (p-trend<0.001 for MVD and PI) (Fig. 3c).

Preoperative imaging of GBM

We found extent of tumor resection was associated with increased patient overall survival (p=0.005). In particular, tumors that were 100% resected, meaning no residual was seen on the postoperative scans, as well as those that were ≥95% resected were associated with significantly better survival (p=0.001 [hazard ratio (HR)=0.25] and p=0.01 [HR=0.36], respectively) (Fig. 4). The significance disappeared when the total resection was ≥85% (Table 3). There was a significant correlation with biopsy and survival (p=0.01), but the HR was 4.25, indicating a worse outcome in the few patients that underwent biopsy. This may represent a selection bias as patients often underwent biopsy if they were very ill or not stable enough for surgical resection.

A correlation was found between overall tumor area and rate of survival (p=0.04). When the size of the area of necrosis or necrosis/tumor index was compared with HRM levels, indices, or survival, only the MIB index was significantly correlated with necrosis or necrosis/tumor index (p=0.03 and p=0.02, respectively) (Table 4).

GBM tumor markers

GLUT-1 and VEGF staining were significantly associated with survival after controlling for age alone (data not shown). When controlling for both age and the amount of resection, a shorter survival time was seen in the higher-staining group for GLUT-1 (p=0.006 [HR=2.11, 95% CI(1.24–3.59)]) and VEGF (p=0.031 [HR=1.84, 95% CI(1.06–3.21)]). Survival in the higher-staining HIF-1 group was shorter but the difference was not quite significant (p=0.061 [HR=1.66, 95% CI(0.98–2.82) (Fig. 5). CA IX was not significantly associated with the length of survival (p=0.52 [HR=1.19, 95% CI(0.70–2.03)] (Fig. 5). GLUT-1 and

VEGF were highly collinearly related (Pearson r=0.54, p<0.001) and thus were not used in this analysis. There was no significant difference in survival in Cox regression models controlling for age alone or age and the amount of resection to compare the high and low groups, defined by a median cut-point, for MVD and proliferation indices.

DISCUSSION

Authors of previous studies have compared various HRMs, MVD, proliferation, necrosis, and extent of resection to astrocytoma tumor grade and overall survival with conflicting results.19¯26 It is difficult to compare the results directly because different HRMs and methods are used. Our study is the first to combine 4 well-known HRMs and indices of MVD and proliferation compared across 3 tumor grades and with the length of survival within the GBM tumor group. Our results show that GLUT-1, VEGF and indices for MVD and proliferation can differentiate tumor grade. Furthermore, GLUT-1 and VEGF were significantly associated with overall survival within the group of patients with GBM.

HRMs, tumor grade, and survival

Various HRMs have been evaluated to review their level of expression in different regions of tumors, across tumor grades, and in association with survival. Abdulrauf et al.30 reported that increased levels of VEGF staining in individuals with LGG correlated with a shorter survival time and increased chance of malignant transformation, whereas Korkolopoulou et al.4 found increased VEGF and HIF-1α staining correlated with shortened survival, but also noted that the significant difference disappeared when the grades were separated and reevaluated. Increased CA IX expression has also been associated with histologic grade and decreased overall survival across tumor grades.31

Although we did not assess the association between the HRMs and overall survival in patients with LGG or AA, the results from the patients with GBM combined with our recent xenograph model of glioma growth15 suggest that GLUT-1 and the glycolytic pathway may play an important role. The adaptive process seen when hypoxia causes a metabolic shift from oxidative metabolism to glycolysis was proposed by Warburg in 1956, and recent correlations between glycolysis and HIF-1 have been reported in various cell types.32¯34 Thus, we believe a focus on the glycolytic pathway may be more beneficial. Recent treatment options that have focused on anti-angiogenic or anti-VEGF therapy have yielded mixed results. It may be that GLUT-1 plays an increased role in the transformation between tumor grades and the aggressiveness of GBM tumors compared with VEGF.

MVD, proliferation, tumor grade, and survival

Reported results are divided as to whether markers of MVD and proliferation can predict transformation from LGG to GBM tumors and correlate with overall survival. Different markers for evaluating MVD, including Factor 8, CD105, and CD31, and various ways of evaluating vascular morphology have been reported. Leon et al.21 found that microvessel counts ≥70 correlated with significantly shorter survival across tumor grades. After age and grade were controlled, branching counts of the vessels have been correlated with survival, but the quantification of MVD has not.2 Sallinen et al.35 have shown that PI may be a better predictor of outcome than histological grade. McKeever et al.22 found that increased MIB index correlated with shorter survival in individuals with LGG; however, others have not found this correlation between proliferation and survival.23, 25

We found that as tumor grade increases to AA and GBM tumors from LGG so does MVD. Interestingly, there was a difference in the final differentiation into high-grade glioma when evaluating proliferation. No correlation between MVD or proliferation and survival in the

GBM group was found. This suggests that increased vascularity is a step towards development of higher-grade tumors but does not play a role in the biological behavior of a given GBM tumor. Although GBM tumors are more vascular than lower-grade tumors, the low-grade astrocytomas have been shown to incorporate pre-existing vessels, whereas GBM tumors develop new vessels.[36, 37] As tumors increase in size, chaotic microvasculature develops that is functionally inefficient compared with normal brain tissue and leads to hypoxic regions within the tumor. In fact, one might imagine that an "angiogenic switch" is one of the defining features of the transformation from LGG to AA and proliferation comes subsequently.

Preoperative imaging, tumor markers, and survival in GBM

MRI_2D was created to increase the speed, accuracy, and precision of brain tumor analysis. MRI_2D provides the researcher with a more standardized approach to image analysis. It allows for the reliable delineation of the enhancing and necrotic regions of tumors when the tumor borders may be unclear to the human eye. MRI_2D also facilitates consistency among the set of images and has hot-keys and layout options that allow the program to perform 5 times faster than previous methods. The use of this program increased our precision because the researcher evaluating the MR images could not arbitrarily include darker/lighter regions on subsequent slides that may be more ambiguous. Accuracy of this program still relies on the researcher's initial limit settings, but the program maintains that accuracy throughout the rest of the images for each patient.

Increased intratumoral necrosis and peritumoral edema visible on preoperative imaging studies has been shown to correlate with poorer overall patient survival.[38-40] Other authors have shown that several preoperative imaging features of GBMs are meaningful predictors of survival. Pope et al.[41] found that the combination of noncontrast-enhancing tumor, absent edema, and no satellite or multifocal lesions corresponded with a doubling of the median survival compared with other combinations. These imaging features have the potential to help determine prognosis of patients in routine clinical practice. Our results demonstrated a correlation of MIB index and both the area of necrosis and the necrosis/tumor index. The significance of this is unclear, however, as we were unable to demonstrate a relationship between either the PI or the area of necrosis and survival. Nevertheless, further work on developing preoperative imaging to predict outcome for patients with GBM is warranted.

Conclusions

The prognosis for individuals diagnosed with GBM tumors remains poor. Identifying means to improve initial prognosis or to recognize individuals in whom augmented therapy would be beneficial has proven difficult. Our results agree with those of other authors that the extent of resection can improve survival only up to a point (≥95% resection). Our results also suggest that MVD and proliferation may play an important role in the transformation from LGG to GBM but do not have as much effect on survival as do the effects of the resulting hypoxia and its downstream effects. Our next step will be to knock-down GLUT-1 in a xenographic model of GBM to evaluate its independent effects on tumor growth as well as its effects in concert with HIF-1α and VEGF. Our study suggests that more research targeting the glycolytic pathway through GLUT-1 may result in a target for effective treatment with a resulting increase in the overall survival in patients with GBM.

Acknowledgments

We thank Sheryl Tripp for assistance with the immunohistochemistry methods and Kristin Kraus for her editorial assistance.

Grant support: This project was supported by a T32 NIH-NCI–Multidisciplinary Cancer Research Training Grant, a GCRC grant for Biostatistical Core support, and a Primary Children's Medical Center Foundation Award to J.R.F., and a Huntsman Cancer Institute funding award to R.L.J.

References

1. Baek JH, Jang JE, Kang CM, Chung HY, Kim ND, Kim KW. Hypoxia-induced VEGF enhances tumor survivability via suppression of serum deprivation-induced apoptosis. Oncogene. 2000; 19(40):4621–31. [PubMed: 11030151]
2. Korkolopoulou P, Patsouris E, Kavantzas N, Konstantinidou AE, Christodoulou P, Thomas-Tsagli E, et al. Prognostic implications of microvessel morphometry in diffuse astrocytic neoplasms. Neuropathol Appl Neurobiol. 2002; 28(1):57–66. [PubMed: 11849564]
3. Sobhanifar S, Aquino-Parsons C, Stanbridge EJ, Olive P. Reduced expression of hypoxia-inducible factor-1alpha in perinecrotic regions of solid tumors. Cancer Res. 2005; 65(16):7259–66. [PubMed: 16103077]
4. Korkolopoulou P, Patsouris E, Konstantinidou AE, Pavlopoulos PM, Kavantzas N, Boviatsis E, et al. Hypoxia-inducible factor 1alpha/vascular endothelial growth factor axis in astrocytomas. Associations with microvessel morphometry, proliferation and prognosis. Neuropathol Appl Neurobiol. 2004; 30(3):267–78. [PubMed: 15175080]
5. Vaupel P, Kelleher DK, Hockel M. Oxygen status of malignant tumors: pathogenesis of hypoxia and significance for tumor therapy. Semin Oncol. 2001; 28(2 Suppl 8):29–35. [PubMed: 11395850]
6. Yetkin FZ, Mendelsohn D. Hypoxia imaging in brain tumors. Neuroimaging Clin N Am. 2002; 12(4):537–52. [PubMed: 12687910]
7. Brat DJ, Mapstone TB. Malignant glioma physiology: cellular response to hypoxia and its role in tumor progression. Ann Intern Med. 2003; 138(8):659–68. [PubMed: 12693889]
8. Lal A, Peters H, St Croix B, Haroon ZA, Dewhirst MW, Strausberg RL, et al. Transcriptional response to hypoxia in human tumors. J Natl Cancer Inst. 2001; 93(17):1337–43. [PubMed: 11535709]
9. Kietzmann T, Krones-Herzig A, Jungermann K. Signaling cross-talk between hypoxia and glucose via hypoxia-inducible factor 1 and glucose response elements. Biochem Pharmacol. 2002; 64(5-6): 903–11. [PubMed: 12213585]
10. Carroll VA, Ashcroft M. Targeting the molecular basis for tumour hypoxia. Expert Rev Mol Med. 2005; 7(6):1–16. [PubMed: 15831177]
11. Mazure NM, Brahimi-Horn MC, Berta MA, Benizri E, Bilton RL, Dayan F, et al. HIF-1: master and commander of the hypoxic world. A pharmacological approach to its regulation by siRNAs. Biochem Pharmacol. 2004; 68(6):971–80. [PubMed: 15313390]
12. Kaur B, Khwaja FW, Severson EA, Matheny SL, Brat DJ, Van Meir EG. Hypoxia and the hypoxia-inducible-factor pathway in glioma growth and angiogenesis. Neuro-oncol. 2005; 7(2): 134–53. [PubMed: 15831232]
13. Maxwell PH, Dachs GU, Gleadle JM, Nicholls LG, Harris AL, Stratford IJ, et al. Hypoxia-inducible factor-1 modulates gene expression in solid tumors and influences both angiogenesis and tumor growth. Proc Natl Acad Sci U S A. 1997; 94(15):8104–9. [PubMed: 9223322]
14. Maxwell PH, Pugh CW, Ratcliffe PJ. Activation of the HIF pathway in cancer. Curr Opin Genet Dev. 2001; 11(3):293–9. [PubMed: 11377966]
15. Gillespie DL, Whang K, Ragel BT, Flynn JR, Kelly DA, Jensen RL. Silencing of hypoxia inducible factor-1α by RNA interference attenuates human glioma cell growth in vivo. Clin Cancer Res. 2007; 13(8):2441–8. [PubMed: 17438103]
16. Heesters MA, Koudstaal J, Go KG, Molenaar WM. Analysis of proliferation and apoptosis in brain gliomas: prognostic and clinical value. J Neurooncol. 1999; 44(3):255–66. [PubMed: 10720205]
17. Kleihues P, Louis DN, Scheithauer BW, Rorke LB, Reifenberger G, Burger PC, et al. The WHO classification of tumors of the nervous system. J Neuropathol Exp Neurol. 2002; 61(3):215–25. discussion 26-9. [PubMed: 11895036]
18. Sharma S, Sharma MC, Sarkar C. Morphology of angiogenesis in human cancer: a conceptual overview, histoprognostic perspective and significance of neoangiogenesis. Histopathology. 2005; 46(5):481–9. [PubMed: 15842629]

19. Behrem S, Zarkovic K, Eskinja N, Jonjic N. Endoglin is a better marker than CD31 in evaluation of angiogenesis in glioblastoma. Croat Med J. 2005; 46(3):417–22. [PubMed: 15861521]
20. Kleinschmidt-DeMasters BK, Meltesen L, McGavran L, Lillehei KO. Characterization of glioblastomas in young adults. Brain Pathol. 2006; 16(4):273–86. [PubMed: 17107596]
21. Leon SP, Folkerth RD, Black PM. Microvessel density is a prognostic indicator for patients with astroglial brain tumors. Cancer. 1996; 77(2):362–72. [PubMed: 8625246]
22. McKeever PE, Strawderman MS, Yamini B, Mikhail AA, Blaivas M. MIB-1 proliferation index predicts survival among patients with grade II astrocytoma. J Neuropathol Exp Neurol. 1998; 57(10):931–6. [PubMed: 9786243]
23. Moskowitz SI, Jin T, Prayson RA. Role of MIB1 in predicting survival in patients with glioblastomas. J Neurooncol. 2006; 76(2):193–200. [PubMed: 16234986]
24. Preusser M, Heinzl H, Gelpi E, Schonegger K, Haberler C, Birner P, et al. Histopathologic assessment of hot-spot microvessel density and vascular patterns in glioblastoma: Poor observer agreement limits clinical utility as prognostic factors: a translational research project of the European Organization for Research and Treatment of Cancer Brain Tumor Group. Cancer. 2006; 107(1):162–70. [PubMed: 16721804]
25. Rodriguez-Pereira C, Suarez-Penaranda JM, Vazquez-Salvado M, Sobrido MJ, Abraldes M, Barros F, et al. Value of MIB-1 labelling index (LI) in gliomas and its correlation with other prognostic factors. A clinicopathologic study. J Neurosurg Sci. 2000; 44(4):203–9. [PubMed: 11327289]
26. Yao Y, Kubota T, Takeuchi H, Sato K. Prognostic significance of microvessel density determined by an anti-CD105/endoglin monoclonal antibody in astrocytic tumors: comparison with an anti-CD31 monoclonal antibody. Neuropathology. 2005; 25(3):201–6. [PubMed: 16193836]
27. Weidner N, Semple JP, Welch WR, Folkman J. Tumor angiogenesis and metastasis--correlation in invasive breast carcinoma. N Engl J Med. 1991; 324(1):1–8. [PubMed: 1701519]
28. Sankoh AJ, Huque MF, Dubey SD. Some comments on frequently used multiple endpoint adjustment methods in clinical trials. Stat Med. 1997; 16(22):2529–42. [PubMed: 9403954]
29. Grambsch P, Therneau TM. Proportional hazards tests and diagnostics based on weighted residuals. Biometrika. 1994; 81:515–26.
30. Abdulrauf SI, Edvardsen K, Ho KL, Yang XY, Rock JP, Rosenblum ML. Vascular endothelial growth factor expression and vascular density as prognostic markers of survival in patients with low-grade astrocytoma. J Neurosurg. 1998; 88(3):513–20. [PubMed: 9488306]
31. Korkolopoulou P, Perdiki M, Thymara I, Boviatsis E, Agrogiannis G, Kotsiakis X, et al. Expression of hypoxia-related tissue factors in astrocytic gliomas. A multivariate survival study with emphasis upon carbonic anhydrase IX. Hum Pathol. 2007; 38(4):629–38. [PubMed: 17367605]
32. Rempel A, Mathupala SP, Griffin CA, Hawkins AL, Pedersen PL. Glucose catabolism in cancer cells: amplification of the gene encoding type II hexokinase. Cancer Res. 1996; 56(11):2468–71. [PubMed: 8653677]
33. Warburg O. On the origin of cancer cells. Science. 1956; 123(3191):309–14. [PubMed: 13298683]
34. Robey IF, Lien AD, Welsh SJ, Baggett BK, Gillies RJ. Hypoxia-inducible factor- 1alpha and the glycolytic phenotype in tumors. Neoplasia. 2005; 7(4):324–30. [PubMed: 15967109]
35. Sallinen PK, Haapasalo HK, Visakorpi T, Helen PT, Rantala IS, Isola JJ, et al. Prognostication of astrocytoma patient survival by Ki-67 (MIB-1), PCNA, and S-phase fraction using archival paraffin-embedded samples. J Pathol. 1994; 174(4):275–82. [PubMed: 7884589]
36. Blouw B, Song H, Tihan T, Bosze J, Ferrara N, Gerber HP, et al. The hypoxic response of tumors is dependent on their microenvironment. Cancer Cell. 2003; 4(2):133–46. [PubMed: 12957288]
37. Folkerth RD. Histologic measures of angiogenesis in human primary brain tumors. Cancer Treat Res. 2004; 117:79–95. [PubMed: 15015553]
38. Barker FG 2, Davis RL, Chang SM, Prados MD. Necrosis as a prognostic factor in glioblastoma multiforme. Cancer. 1996; 77(6):1161–6. [PubMed: 8635139]
39. Hammoud MA, Sawaya R, Shi W, Thall PF, Leeds NE. Prognostic significance of preoperative MRI scans in glioblastoma multiforme. J Neurooncol. 1996; 27(1):65–73. [PubMed: 8699228]

40. Lacroix M, Abi-Said D, Fourney DR, Gokaslan ZL, Shi W, DeMonte F, et al. A multivariate analysis of 416 patients with glioblastoma multiforme: prognosis, extent of resection, and survival. J Neurosurg. 2001; 95(2):190–8. [PubMed: 11780887]

41. Pope WB, Sayre J, Perlina A, Villablanca JP, Mischel PS, Cloughesy TF. MR imaging correlates of survival in patients with high-grade gliomas. AJNR Am J Neuroradiol. 2005; 26(10):2466–74. [PubMed: 16286386]

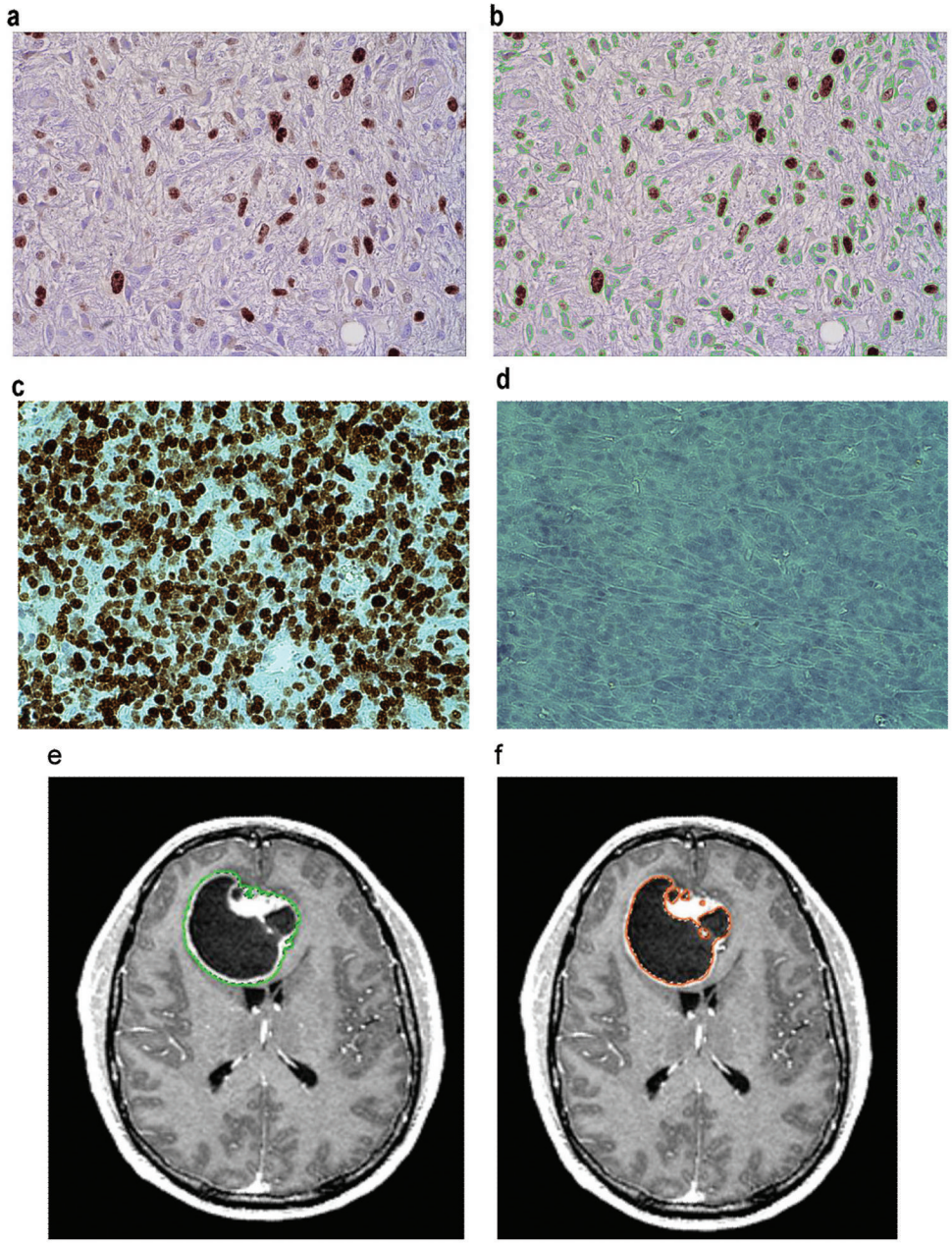

FIGURE 1.

(a,b) Photomicrographs showing MIB-1 staining of GBM tumor cells. Brown staining indicates the MIB-1 stained cells. In b, green lines surround the brown cells plus the blue cells (background-stained). Proliferation index=(brown stained cells)/(brown+blue stained cells)×100. (c,d) Photomicrographs of positive (human thymus) and negative controls for MIB staining. (e,f) Axial T1-weighted contrast-enhanced MR images. In e, a green line surrounds the contrast-enhancing tumor region. In f, the orange surrounds the regions of necrosis (dark).

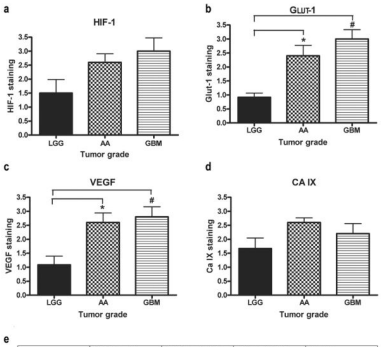

e

	LGG vs. AA	LGG vs. GBM	AA vs. GBM	Trend
HIF-1	0.16	0.15	0.27	0.023
GLUT-1	0.006	0.001	0.24	<0.001
VEGF	0.015	0.011	0.60	0.002
CA IX	0.1	0.41	0.37	0.18

FIGURE 2.

HRMs compared across tumor grades. (a) No significant differences were seen when HIF-1 staining was compared across tumor grades. (b) GLUT-1 staining was significantly different when LGG was compared with AA and GBM. (c) VEGF staining was significantly different when LGG was compared with AA and GBM. (d) No significant differences were seen when CA IX staining was compared across tumor grades. (e) Table of p-values of HRMs compared across tumor grades and the p-values for the trends (light grey, $p<0.05$; dark grey, $p<0.01$).

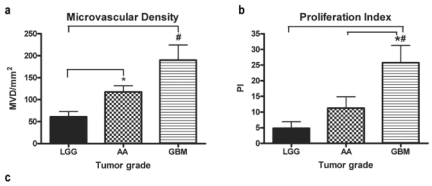

c

	LGG vs. AA	LGG vs. GBM	AA vs. GBM	Trend
MVD	0.027	0.003	0.09	<0.001
PI	0.19	0.001	0.038	<0.001

FIGURE 3.

Indices compared across tumor grades. (a) MVD was significantly different when LGG was compared with AA and GBM. (b) PI was significantly different when LGG and AA compared with GBM. (c) Table of p-values of indices compared across tumor grades and the p-values for the trends (light grey, $p<0.05$; dark grey, $p<0.01$).

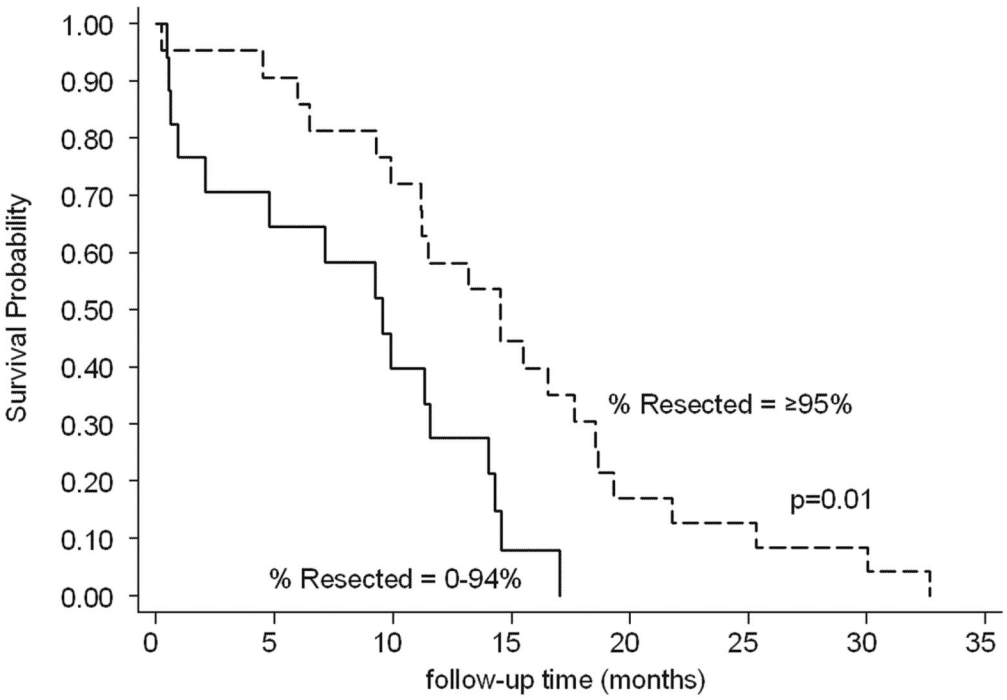

FIGURE 4.
Age-adjusted Kaplan-Meier survival curve when %Resected is divided at ≥95%.

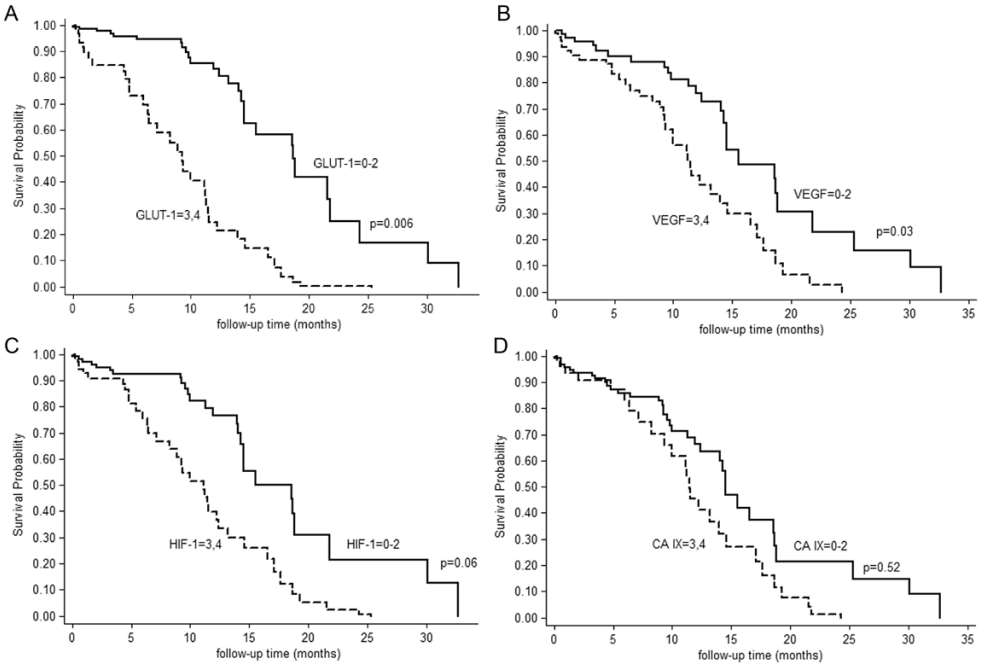

FIGURE 5.

Age-adjusted Kaplan-Meier survival curves when HRMs are divided at the median (0–2 or 3–4). (a) GLUT-1; (b) VEGF; (c) HIF-1; (d) CA IX.

TABLE 1

Characteristics of patients with GBM tumors

Patient characteristics	No. patients in cohort (%)	No. patients in imaging subset (%)
Overall	62	42 (67.75)
Sex		
Male	42 (67.74)	30 (71.43)
Female	20 (32.26)	12 (28.57)
Age		
Mean±SD (range)	62.47±11.26 (40.7–81.2)	63.5±11.38 (40.7–81.2)
Extent of surgery		
Biopsy	6 (9.68)	0
Subtotal resection	40 (64.52)	16 (38.10)
Gross total resection (≥95%)	16 (25.81)	26 (61.90)
Side		
Right	29 (46.77)	20 (47.62)
Left	30 (48.39)	20 (47.62)
Bilateral	3 (4.84)	2 (4.76)
Location		
Frontal	19 (30.65)	12 (28.57)
Occipital	5 (8.06)	3 (7.14)
Temporal	24 (38.71)	18 (42.86)
Parietal	12 (19.35)	8 (19.05)
Thalamus	2 (3.23)	1 (2.38)
Awake cortical mapping		
Yes	11 (17.74)	11 (26.19)
No	51 (82.26)	31 (73.81)
Chemotherapy treatment		
Yes	44 (70.97)	31 (73.81)
No	15 (24.19)	8 (19.05)
Unknown	3 (4.84)	3 (4.76)
Radiotherapy treatment		
Yes	50 (80.65)	34 (80.95)
No	11 (17.74)	7 (16.67)
Unknown	1 (1.61)	1 (2.38)
Progression-free survival in mo±SD (range)	5.56±4.99 (0.56–24.3)	5.84±5.50 (0.56–24.3)
Overall survival in mo±SD (range)	10.77±7.58 (0.07–32.65)	11.26±7.87 (0.26–32.65)

TABLE 2

Characteristics of patients with 3 grades of gliomas

	Total	LGG (WHO grade II)	AA (WHO grade III)	GBM (WHO grade IV)
No. patients	32	12	10	10
Mean age in years (SD)	50.99 (18.29)	37.92 (16.92)	54 (16.37)*	63.68 (10.84)#
Sex: no. (%)				
Male	22 (68.75)	9 (75)	5 (50)	8 (80)
Female	10 (31.25)	3 (25)	5 (50)	2 (20)

* p=0.04.

# p<0.001.

TABLE 3

Amount of resection compared with survival.

	No. patients (%)	Median survival in mo (95%CI)	p-value for survival (controlling for age) [Hazard ratio]
GTR=100% (n=38)		15.52 (11.24–18.64)	p=0.001 [HR=0.25]
Yes	19 (50.00)		
No	19 (50.00)		
GTR≥95% (n=38)		14.53 (11.15–17.65)	p=0.01 [HR=0.36]
Yes	23 (60.53)		
No	15 (39.47)		
GTR≥85% (n=38)		13.18 (9.93–15.52)	p=0.09
Yes	29 (76.32)		
No	9 (23.68)		
Biopsy		1.38 (0.95–2.22)	p=0.01 [HR=4.25]
Yes	4 (9.52)		
No	38 (90.48)		

GTR, gross total resection.

Four patients with biopsies were not included in the comparisons of GTR=100%, GTR≥95%, and GTR≥85%.

TABLE 4

P-values comparing HRMs, MVD, PI, and survival with tumor area, necrosis area, and necrosis/tumor index

	Tumor area (p-value)	Necrosis area (p-value)	Necrosis/tumor index (p-value)
HIF-1	0.10	0.16	0.45
GLUT-1	0.16	0.21	0.50
VEGF	0.62	0.68	0.82
CA IX	0.07	0.06	0.21
MVD	0.57	0.77	0.56
PI	0.31	**0.03**	**0.02**
Survival	**0.04**	0.19	0.67

Bold indicates significant relationship.